



REVIEW

## Recent Progress of Surface Passivation Molecules for Perovskite Solar Cell Applications

Baohua Zhao<sup>1</sup>, Teng Zhang<sup>2,\*</sup>, Wenwen Liu<sup>2</sup>, Fansong Meng<sup>2</sup>, Chengben Liu<sup>1</sup>, Nuo Chen<sup>2</sup>, Zhi Li<sup>3</sup>, Zhaobin Liu<sup>3</sup> and Xiyou Li<sup>2,\*</sup>

<sup>1</sup>College of Chemistry and Chemical Engineering, China University of Petroleum (East China), Qingdao, 266580, China

<sup>2</sup>School of Materials Science and Engineering, China University of Petroleum (East China), Qingdao, 266580, China

<sup>3</sup>Shandong Energy Group Co., Ltd., Jinan, 250000, China

\*Corresponding Authors: Xiyou Li. Email: xiyouli@upc.edu.cn; Teng Zhang. Email: tzhangae@connect.ust.hk

Received: 14 April 2022 Accepted: 20 May 2022

### ABSTRACT

Due to the solution processable nature, the prepared perovskite films are polycrystalline with considerable number of defects. These defects, especially defects at interface accelerate the carrier recombination and reduce the carrier collection. Besides, the surface defects also affect the long-term stability of the perovskite solar cells (PVSCs). To solve this problem, surface passivation molecules are introduced at selective interface (the interface between perovskite and carrier selective layer). This review summarizes recent progress of small molecules used in PVSCs. Firstly, different types of defect states in perovskite films are introduced and their effects on device performance are discussed. Subsequently, surface passivation molecules are divided into four categories, and the interaction between the functional groups of the surface passivation molecules and selective defect states in perovskite films are highlighted. Finally, we look into the prospects and challenges in design noble small molecules for PVSCs applications.

### KEYWORDS

Perovskite solar cells; defect; surface passivation; small molecules

## 1 Introduction

After ten years of accumulation, the photoelectric conversion efficiency (PCE) of organic-inorganic perovskite solar cells (PVSCs) has increased from the initial 3.8% [1] to 25.7% [2]. The rapid development is attributed to the excellent photophysical properties [3,4] of the perovskite materials, such as direct bandgap, prominent light absorption coefficient ( $\approx 10^5 \text{ cm}^{-1}$ ), and long carrier diffusion length ( $>1 \mu\text{m}$ ) [5,6]. Although progressive achievement has been witnessed, the achievable PCE is still far lower than the theoretical Shockley-Queisser (S-Q) limit, mainly due to the non-radiative recombination [7]. To be honest, non-radiative recombination is inevitable in photovoltaic devices. While developing methods and strategies to reduce the non-radiative recombination are always a hot topic in the photovoltaic field.

The non-radiative recombination is largely defect contributed. To be more specific, the more defect states in the device, the more severe the non-radiative recombination and inferior PCE. Take the open-



circuit voltage ( $V_{oc}$ ) as an example, the  $V_{oc}$  originates from the quasi-Fermi level of electron and hole in the light-excited photo-absorber. The defect state in the photo-absorber would trap part of the carriers and cause non-radiative recombination, reducing the steady-state carrier density [8,9]. Therefore, the splitting of the quasi-Fermi level would be reduced, reducing the achievable  $V_{oc}$  [10]. As for perovskite, they are polycrystalline films prepared by a low-temperature solution process. Non-negligible defects (such as dangling bond, vacancies, interstitials, and antisites) can be expected at the perovskite bulk, grain boundaries and interfaces [11–13]. Although theoretical investigation suggests most bulk defects are shallow defects which don't result in carrier recombination [14,15], the defects at interface are different. It was found that the defect density of the PVSCs is in the order of  $\sim 10^{18} \text{ cm}^{-3}$ , much higher than that of single crystals [16]. This suggests surface defects instead of bulk defects are the dominant defect in PVSCs. Besides, some of the defect species, iodide vacancy ( $V_I$ ) for example, which are benign in the bulk, turn into recombination center at surface [17,18]. The situation can be worse taking the different chemical environment near interface into consideration [19,20].

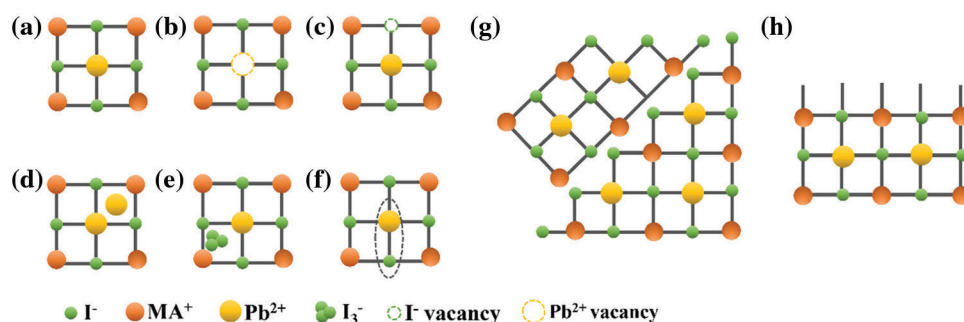
Surface passivation which introduces suitable materials at perovskite/carrier selective interface (CSL), can heal deep defects at interface. Non-radiative recombination can be reduced, effective charge carrier can be guaranteed and improved PCE is achieved. At present, different kinds of materials including inorganic materials [21–25], small molecules [26–32] and polymers [33–35] are selected for surface passivation. Among them, the small molecule is most widely used. This is because the small molecule can be adjusted according to the species of defects [36]. While more effective surface passivation molecules are needed to reduce the  $V_{oc}$  loss of PVSCs. In this review, since the non-radiative recombination is defect contributed, we start with a general description of the defect states in PVSCs. The type and chemical nature of selective defects are discussed. The influence of defects during the carrier transporting process are highlighted. Next, we summarize some of the most widely used surface passivation molecules. The interaction between different defects and surface passivation molecules are described in detail. Due to the complexity of defect states at the perovskite/CSL interface, there might still be a long way in developing effective surface passivation molecules. At last, we talk about the problems, challenges and strategies in developing effective surface passivation molecules for PVSCs approaching the theoretical limit.

## 2 Defects in PVSCs

Since most of the perovskite films used for PVSCs are low temperature solution processed, the perovskite precursor undergoes fast nucleation and crystallization, so it is difficult to prepare well-ordered and defect-free perovskite films. The defect density of the polycrystalline perovskite films is approximately five orders of magnitudes higher than that of single crystal perovskite and conventional crystalline silicon [10,37–41]. Thus a detailed and comprehensive understanding of the defect properties will be essential for developing high-performance PVSCs.

### 2.1 Defects in Perovskite

The crystal structure of the organic-inorganic perovskite  $ABX_3$  is composed by B (central metal ion:  $Pb^{2+}$ ,  $Sn^{2+}$ ) and X (halogen ion:  $Cl^-$ ,  $Br^-$ , or  $I^-$ ) forming  $BX_6^{4-}$  corner-sharing octahedra, the cubic octahedral cavity is occupied by the A cations ( $(MA^+; CH_3NH_3^+)$ ,  $(FA^+; HC(NH_2)_2^+)$ ). However, this is the ideal case. Imperfect lattices such as vacancies, interstitials, and antisites inevitably exist in the perovskite crystals [42,43]. As shown in Fig. 1, the defects in perovskite crystals can be classified as follows: vacancy ( $V_A$ ,  $V_B$ ,  $V_X$ ), interstitial ( $B_i$ ,  $X_i$ ) and antisites ( $Pb_i$ ,  $I_{Pb}$ ). At the same time, at the surface or grain boundary, the lattice is suddenly interrupted, resulting in a large numbers of non-coordinating ions and dangling bonds.



**Figure 1:** Schematic illustration of typical defects in PVSCs: (a) perfect lattice, (b)  $\text{Pb}^{2+}$  vacancies, (c)  $\text{I}^-$  vacancies, (d) interstitial  $\text{Pb}^{2+}$ , (e) interstitial  $\text{I}_3^-$ , (f) Pb-I antisite substitution, (g) grain boundary, and (h) dangling bonds on the surface

## 2.2 The Impact of Defects

The optoelectronic properties of the perovskite films are largely determined by the defect states [44]. Starting with the band structure, the valance band maximum (VBM) of the organic-inorganic perovskite is mainly composed of Pb s and I p anti-bonding states, and the conduction band minimum (CBM) consists of a Pb p state [45]. The defect states will possibly bring extra band state into the band gap and alter the conductivity of the semiconductors. The conductivity of the perovskite films can be well tuned from p-type to n-type through defect engineering [46]. The MAI-rich and  $\text{PbI}_2$ -rich perovskite films are p and n self-doped, respectively. Depending on the growth condition, the carrier concentration (defect density) of the prepared films varied as much as six orders of magnitude [46].

In terms of photophysics, the defect states can be classified into shallow-level defects and deep-level defects depending on their energy states. If the energy state of the defects is located near the band edges (VBM/CBM), this kind of defects can be named as shallow defect, while deep defects are located at intermediate transition levels within the band gap, only the latter (deep defect) is responsible for the non-radiative recombination. Taking the widely used methylamine lead iodide ( $\text{MAPbI}_3$ ) as an example, theoretical investigation suggests the bulk defects of the  $\text{MAPbI}_3$  with low formation energy ( $\text{I}_i$ ,  $\text{MA}_{\text{Pb}}$  and  $\text{V}_{\text{MA}}$ ) are shallow defect, this explains the long carrier diffusion length of the perovskite films [47,48]. While due to different local chemical environment at surface, deep defects show up at surface. According to a recent study by Huang, deep defect favored the surface instead of the bulk [37]. Agiorgousis et al. suggested the uncoordinated  $\text{Pb}^{2+}$  at surface tended to form Pb clusters, which was deep defect with low formation energy [49]. Taufique et al. [50] suggested anti-site defects ( $\text{Pb}_i$  and  $\text{I}_{\text{Pb}}$  for example) were deep defect, since anti-site defects introduced new bonds between the defect atoms and other chemicals, thereby forming electron trap states in the bandgap region. During the two-step preparation process of the perovskite films, a Pb-rich environment can be expected at surface, this greatly reduces the formation energy of the  $\text{Pb}_i$  deep defect [51–53]. These deep defects with low formation energies act as Shockley-Reid-Hall non-radiative recombination centers, which lead to non-radiative recombination of free electrons and holes, resulting in the loss of  $V_{\text{oc}}$  and seriously affecting the performance of the device [54].

In addition to the energy loss, the presence of defects can also have other adverse effects on the device characterization [55]. Due to the soft nature of perovskite materials, charged defects move with the assistance of an electric field [56]. This phenomenon is called ion migration [57,58]. Under an electric field, positively charged point defects with low activation energy tend to move toward the cathode, while negatively charged defects diffuse to the anode [59,60]. The ion migration tendency is highly dependent on light and temperature [61–63]. In 2016, Xing et al. found that the ion drift velocity of polycrystalline  $\text{MAPbI}_3$  film under 1 sun was an order of magnitude higher than that under dark conditions [62]. This proved that illumination can greatly reduce the active energy of ion migration. The hysteresis behavior of the current density-voltage (J-V) curves

of PVSCs under different scanning directions (forward and reverse scan) is also believed to be caused by ion migration [63,64]. As charged defects with high mobility under working conditions, will lead to the defect accumulation and band bending at the perovskite-carrier transport layer interface [65].

The poor stability of the PVSCs has been regarded as the main obstacle hindering their commercialization [66]. Taking MAPbI<sub>3</sub> as an example, the decomposition process can be expressed by the following chemical equation [67]:



The existence of surface and bulk defects also accelerates the degradation of perovskite materials in air and thermal environments [68,69]. The degradation of PVSCs starts from grain boundaries (GBs), and then gradually decomposes into irreversible products [70–72]. Ahn et al. found that charges which were trapped by the defect states at interface, can trigger the irreversible degradation of PVSCs under light and moisture [73]. Besides moisture, V<sub>I</sub> exposed at surface tends to bond with oxygen, speeding up the reaction between reactive superoxide (O<sub>2</sub><sup>•−</sup>) and MA<sup>+</sup>. It is demonstrated that high-quality perovskite films with large grain size, less defect density exhibited lower density of O<sub>2</sub><sup>•−</sup> [74].

Since the PCE is defect related and the stability of the devices is also largely contributed by defects, it is necessary to suppress the defect related deleterious effects including nonradiative recombination, charge trapping, ion transport, as well as hysteresis and device degradation. Thus, defect passivation strategy can speed up the development of long-term stable, reliable, and efficient PVSCs.

### 3 Surface Passivation Molecule

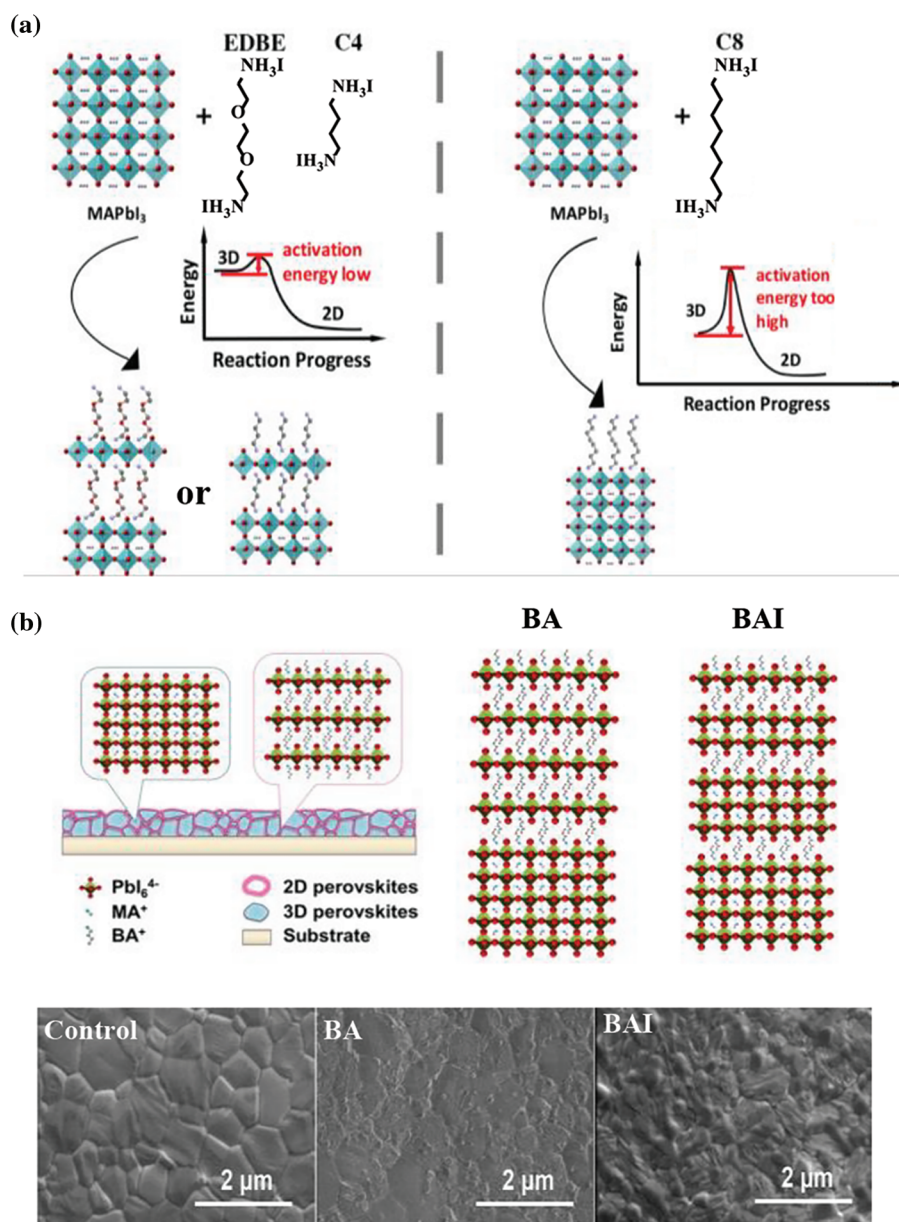
Since the poor interface has been regarded as the main reason for the unsatisfied PCE of PVSCs, introducing small molecule to reduce the chemical activity of the perovskite/CSL interface could be a solution [21,35,75,76]. While the effectiveness of surface passivation molecule is highly dependent on its structure [77–79]. In other words, the interaction between surface passivation molecule and selective defect on the surface. So far, alkylamine halides, Lewis bases, Lewis acids and multifunctional molecules are used, increased performance can be achieved by forming ionic bonds, coordination bonds and supramolecular halogen bonds.

#### 3.1 Passivation with Organic Amines and Their Halides

Inspired from methylamine cation, alkyl amine and its halide are the most commonly used surface passivation molecule for PVSCs. At present, organic amines such as ethylamine (EA) [80], n-butylamine (BA) [81], phenethylamine (PEA) [82], octylamine (OA) [83] and dioctylamine iodide (C8) [84] have been used to passivate the surface defects of PVSCs. For EA, BA with relatively smaller radius, low-dimensional perovskites with improved stability can be expected (Fig. 2a). In 2017, Wang et al. found that BAI constituted a wide bandgap two dimensional (2D) layered perovskite on the three dimensional (3D) perovskite surface [81]. Since the band gap of 2D perovskite is larger than that of 3D perovskite, when the charge reaches this interface from the 3D perovskite grains, they will be reflected and stay in the 3D perovskite without being trapped by surface defects. At the same time, 2D perovskite can alleviate the erosion of water vapor on perovskite films, the 2D perovskite capped devices maintain 80% of their ‘post burn-in’ efficiency after 1000 h in air, and close to 4000 h after encapsulation. Afterwards, Huang et al. suggested that a 2D/3D heterojunction structure can be formed using n-butylamine (BA) and



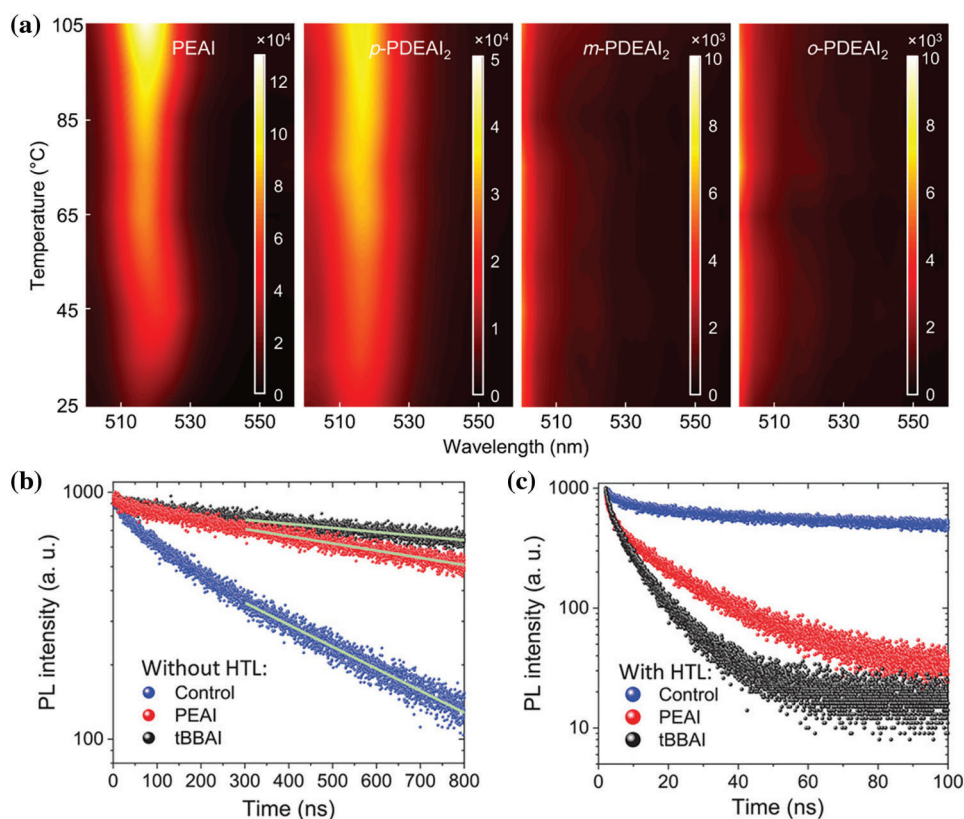
n-butylamine hydroiodate (BAI) as surface passivation molecule [85]. PVSCs with 2D/3D superimposed structure have been proved to effectively improve the device performance via defect passivation and self-healing effects. Compared with the BAI treatment, BA passivated perovskite forms a textured 2D perovskite layer as shown in Fig. 2b. In the end, they reported PVSCs with PCE of 19.29%, which still maintain 96.5% of the original PCE when heated at 95°C for 100 h. While for the large alkylamines (octylamine, OA, etc.), they could not self-assemble into a 2D/3D structure due to higher formation energy, but they can directly act as passivation molecules (Fig. 2a). 2D structure is not observed on the OA armoured perovskite films. Instead, (110) preferred orientation can be expected. This facilitate carrier transportation and an improved stability [83].



**Figure 2:** (a) Schematic diagram of passivation mechanism [84]. Reproduced with permission. Copyright 2016, ACS Energy Letters. (b) Schematic figure of the perovskite film treated by BA to form a 2D/3D stacking structure and SEM images of MAPbI<sub>3</sub> films, BA-treated MAPbI<sub>3</sub> films, and BAI-treated MAPbI<sub>3</sub> films [85]. Reproduced with permission. Copyright 2018, The Journal of Physical Chemistry Letters

Besides alkyl amines, aromatic amine also have a strong interaction with the defect states in the perovskite film [86]. Wang et al. [87] introduced aniline (A), benzylamine (BnA) and phenethylamine (PEA) as surface passivation molecule through a simple post-deposition process, the Voc was increased to 1.12 V, almost the record at that stage. Furthermore, with the assist of grazing-incidence wide angle X-ray scattering (GIWAXS), Hu et al. discovered that compared with BAI, the PEAI could vertically aligned on the surface of the perovskite films, the longitudinal transport of carriers is facilitated [88]. In 2018, Jiang et al. [8] reported a record PCE of 23.32% using PEAI as passivator. After a detailed investigation, they suggested the structure of PEAI passivated perovskite was dependent on the processing condition. 2D structure would not show up without annealing. Moreover, they proved that the room temperature processed PEAI brought the best photoluminescence (PL) density. Simultaneously, the stability of PEAI passivated PVSCs was also improved. Although previous investigation proved 2D perovskite were effective passivator, recent studies suggested they might also be recombination centers [89,90]. To reduce the possibility of 2D perovskite formation, Nazeeruddin et al. selected ortho-(o-), meta-(m-) and para-isomers (p-) of (phenylene)di(ethylammonium) iodide (PDEAI<sub>2</sub>) as surface passivation materials [91]. The results showed that the O-PDEAI<sub>2</sub> effectively increases the energy barrier of the 2D perovskite. Bulky organic cations from entering the perovskite lattice are prevented even at high temperatures as shown in Fig. 3a. The achievable PCE is also influenced by the morphology of the surface passivation molecules on the perovskite surface. Michael Grätzel et al. synthesized a new molecular passivator 4-tert-butyl-benzylammonium iodide (tBBAI), the tert-butyl side group prevented the unnecessary aggregation through steric repulsion [92]. TRPL (Figs. 3b and 3c) confirmed that tBBAI passivated perovskite films exhibit less nonradiative charge carrier recombination. The fill factor (FF) has been increased from 0.75 to 0.82 after introducing tBBAI passivation. In addition, the high hydrophobicity of tBBAI leads to an enhanced moisture resistivity and thus better operational stability.

Furthermore, organic amines with special steric structure are considered as passivator. Since porphyrin and its derivatives have excellent photoelectric properties and thermal stability, Wu et al. introduced a monoammonium zinc porphyrin (ZnP) compound onto the perovskite surface and realized a remarkably enhanced performance for large-area (1.96 cm<sup>2</sup>) PVSCs [93]. In 2021, Cao et al. introduced monoamine porphyrins (MPs, M = Co, Ni, Cu, Zn, or H) into the perovskite films. XRD test (Fig. 4a) confirmed the porphyrin self-assembled into supramolecular structure at the grain boundaries of perovskite films [94]. The time of flight secondary ion mass spectrometry (TOF-SIMS) suggested the superstructure was located at the grain boundary of the perovskite film (Figs. 4b–4d). This porphyrin self-assembled supramolecular realized the rapid transfer of holes, which accelerated the effective extraction of the charges in the devices. Finally, the devices received an efficiency of 22.8% with an active area of 1 cm<sup>2</sup>. Next, a series of new organic passivation molecules with strong hydrophobicity synthesized by Zhao et al. [95]. Here, they started with triarylated amine, the building blocks of Spiro-OMeTAD [96]. Their study showed that PVSCs modified with N-((4-(N,N,N-triphenyl)phenyl) ethyl)ammonium (TPA-PEABr) had the best PCE. The improved performance can be attributed to the defect passivation ability and hydrophobicity of TPA-PEABr. Subsequently, Zhang et al. designed and synthesized 2-(4-ethylaminobenzene)-9,9'-spirobifluorene (BSBF-NH<sub>2</sub>) organic passivated small molecules. With the assistance of femtosecond transient absorption (fs-TA) spectrum, they discovered the extraction rate of holes was reduced from 302 ps to 139 ps after BSBF-NH<sub>2</sub> passivation as shown in Figs. 4e–4g. The enhancement of hole extraction efficiency due to the improved interfacial contact between the perovskite layer and the HTL by introduce BSBF-NH<sub>2</sub>. In addition, the BSBF-NH<sub>2</sub> with an amino group can reduce the density of defect states in perovskite films, reduces the probability of non-radiation recombination. With the assistance of improved contact and defect healing potential, the Voc and FF of PVSCs after BSBF-NH<sub>2</sub> modification are greatly improved. Finally, PVSCs with PCE of more than 20% are successfully prepared. The environmental stability of PVSCs is improved after modification with BSBF-NH<sub>2</sub>, which can be attributed to the hydrophobicity of BSBF-NH<sub>2</sub>.



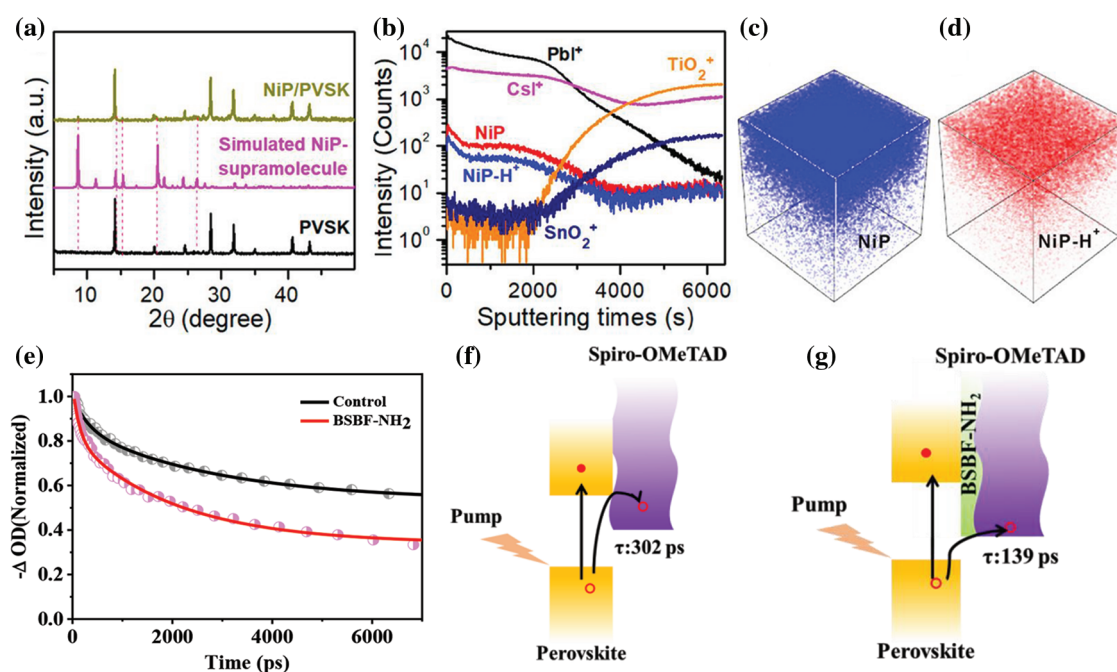
**Figure 3:** (a) Temperature-dependent PL images of the perovskite films treated with the different organic halide salts [91]. Reproduced with permission. Copyright 2021, Nature Communications. (b) TRPL for the layer structure glass/FTO/mp-Al<sub>2</sub>O<sub>3</sub>/perovskite/without surface layer (control, blue), with PEAI (red), and tBBAI (black) [92]. The fitted curves using the model described in the main text are shown by green lines. (c) TRPL measurements of HTL containing samples without interface layer, with PEAI, and with tBBAI [92]. Reproduced with permission. Copyright 2020, Advanced Materials

### 3.2 Passivation of Lewis Base

A Lewis base contains electron-donating atoms such as N-donor, O-donor, S-donor and P-donor, which can effectively passivating positively charged defects (e.g., under-coordinated Pb<sup>2+</sup> and Pb<sup>2+</sup> interstitials) [97]. Thiophene and pyridine were first used for surface passivation [98]. The uncoordinated Pb atoms at grain boundaries can be effectively passivated by thiophene and pyridine (Fig. 5a). The PL lifetimes have been enhanced by nearly an order of magnitude, highlighting the effectiveness of thiophene and pyridine (Fig. 5b). Using time-domain density functional theory combined with nonadiabatic molecular dynamics, He et al. investigated the interaction between Lewis base molecule and the perovskite surface in detail. They discovered that the charge recombination is driven by slow Pb-I vibrations. Besides, bidentate Lewis bases, 2-mercaptopyridine (2-MP) and d-4-tert-butylphenylalanine (D4TBP) for example, are effective surface passivation molecules. Other types of molecules with different functional groups, such as carboxyl groups (C=O) [99,100] and phosphoric acid containing groups (P=O) [101] also exhibit a strong passivation effect on uncoordinated Pb<sup>2+</sup>. In 2018, Chen et al. introduced a hydrophobic organic acid molecule, 4-dimethylaminobenzoic acid (4-DMABA) [102], to modify the top surface of perovskite thin film (Fig. 5c). Fourier transform infrared spectroscopy (FT-IR) showed that the stretching vibration of the C=O bond has shifted from 1666 cm<sup>-1</sup> (4-DMABA) to 1618 cm<sup>-1</sup> (4-DMABA/MAPbI<sub>3</sub>) as shown in Fig. 5d. The shift can be explained by the strong interaction between C=O and Pb<sup>2+</sup>. Ultimately, the PCE of inverted PVSCs has increased from 17.43% to



19.87%. In addition, Yang et al. systematically investigated the effect of theophylline, caffeine, and theobromine as surface passivation molecules [103]. Owing to the strong interaction between theophylline molecule and surface antisite defects, the PCE has been improved from 21% to 22.6% after theophylline passivation. Organic molecules with P=O groups have also been exploited as efficient passivation agents for  $\text{Pb}^{2+}$  defects. Meng and co-workers [101] proved that tribenzylphosphine oxide (TBPO) was an excellent passivator through strong Pb-O coordination and intermolecular  $\pi$ - $\pi$  conjugation, thereby achieving efficient and stable PVSCs. The TBPO can significantly inhibit the deep defects and reduce the attempt-to-escape frequency ( $\nu_0$ ) by two orders of magnitude. Therefore, high efficiency of exceeding 22% with significantly suppressed hysteresis has been achieved. More importantly, the TBPO passivated perovskite films show a higher contact angle, which contribute to significantly enhanced stability.

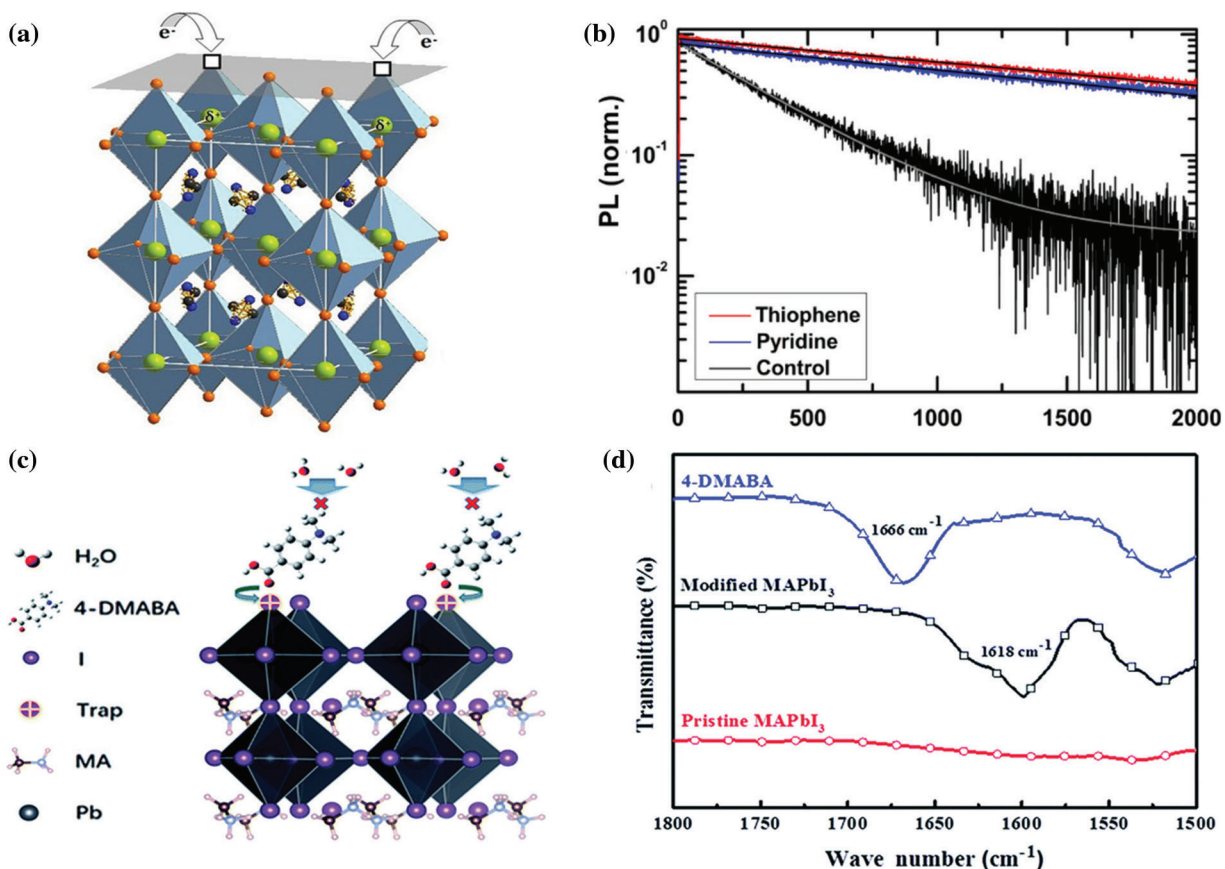


**Figure 4:** (a) XRD of simulated NiP-supramolecule, perovskite samples with and without NiP [94]. (b) Fragments distribution in NiP-doped perovskite film [94]. TOF-SIMS profiles showing (c) NiP and (d) NiP-H<sup>+</sup> components from the top to bottom [94]. Reproduced with permission. Copyright 2021, Journal of the American Chemical Society. (e) Transient band edge bleach kinetics (dot symbols) and their corresponding decay exponential fits (lines) for the perovskite/Spiro-OMeTAD films at 780 nm [96]. Schematic illustration of hole extraction process at the control (f) and BSBF-NH<sub>2</sub> passivation interface (g) [96]. Reproduced with permission. Copyright 2022, Journal of Materials Chemistry C

### 3.3 Passivation of Lewis Acid

Lewis acid refers to molecules or ions that can accept electron pairs. Such molecules can be covalently bonded to form acid-base complexes without electron transfer. Therefore, Lewis acid has a unique passivation potential for negative charged defects, such as free iodide ions and lead iodine antisite defects. The most representative Lewis acid passivator is fullerene ( $\text{C}_{60}$ ) and its derivatives. Due to their inherent electronic attraction ability, they are also good electron transport materials [104–106]. In 2015, Sargent et al. reported the first perovskite-PCBM hybrid solid with significantly reduced hysteresis and less Voc loss [104]. As shown as in Fig. 6a, UV-vis spectroscopy suggests that a peak shows up at

1020 nm for the perovskite-PCBM hybrid solution, which can be attributed to the fact that PC<sub>61</sub>BM molecules receive electrons from iodide. Furthermore, three fullerene derivatives (IC<sub>60</sub>BA, PC<sub>61</sub>BM, and C<sub>60</sub>) with different carrier mobility were considered as surface passivator. C<sub>60</sub> stands out due to the high mobility, as confirmed from PL spectra (Fig. 6b) [107]. Iodopentafluorobenzene (IPFB) is reported to interact with uncoordinated halides effectively and passivate surface anion defects by forming halogen bond (Fig. 6c) [108]. This enhances the charge transfer at the perovskite/HTM interface and increases the carrier lifetime [108].



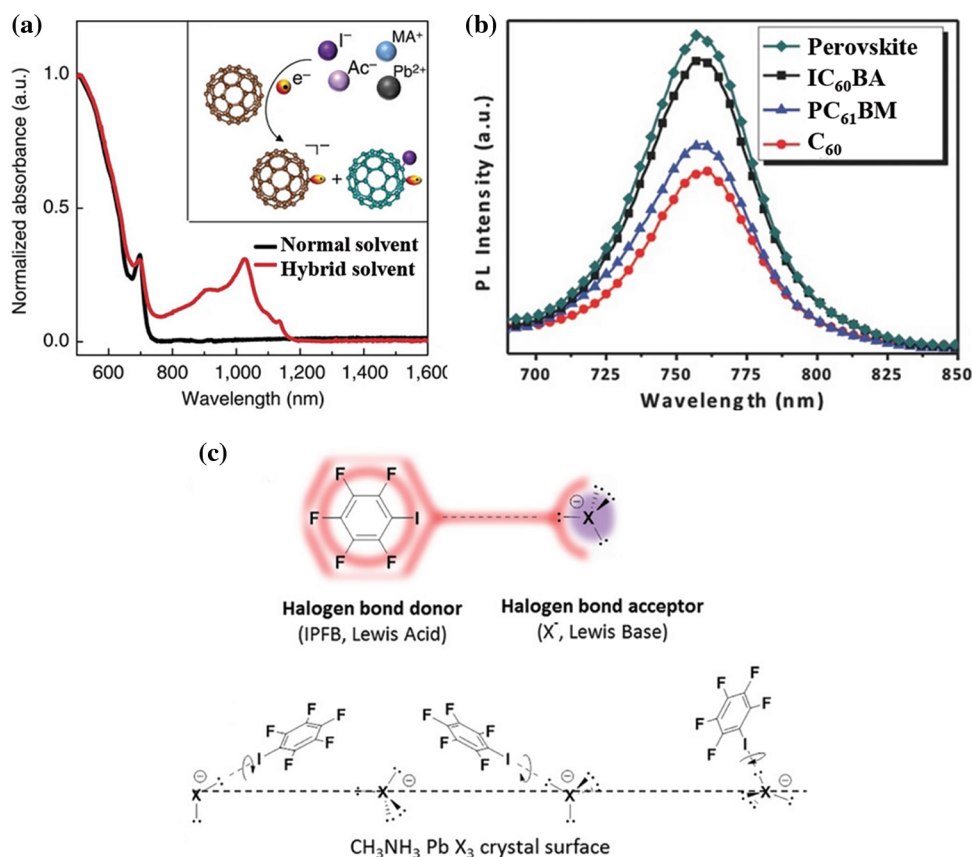
**Figure 5:** (a) Proposed passivation mechanism of thiophene or pyridine [98]. (b) Time-resolved PL measurements of control, thiophene, and pyridine samples with 507 nm pulsed (200 kHz) excitation [98]. Reproduced with permission. Copyright 2014, ACS Nano. (c) Schematic diagram showing the interaction mode of 4-DMABA molecules with MAPbI<sub>3</sub> [102]. (d) FTIR spectra of powder samples of MAPbI<sub>3</sub>, 4-DMABA and a 4-DMABA/MAPbI<sub>3</sub> mixture [102]. Reproduced with permission. Copyright 2018, Journal of Materials Chemistry A

### 3.4 Co-Passivation of Multifunctional Groups

Compared with monofunctional molecules, multifunctional molecules have a stronger synergistic passivation effect [109,110]. Small molecules with carboxyl or carbonyl and amine are firstly considered. Aminovaleric acid (AVA), which contains a carboxyl group and an amine group, has shown to effectively improve the stability of selective devices [111]. Next, Hu et al. [112] combined experimental and theoretical study to explore the effect of natural amino acids (NAAs) passivators. They chose glycine (Gly), glutamic acid (Glu), proline (Pro) and arginine (Arg) as passivation materials. The Arg passivated



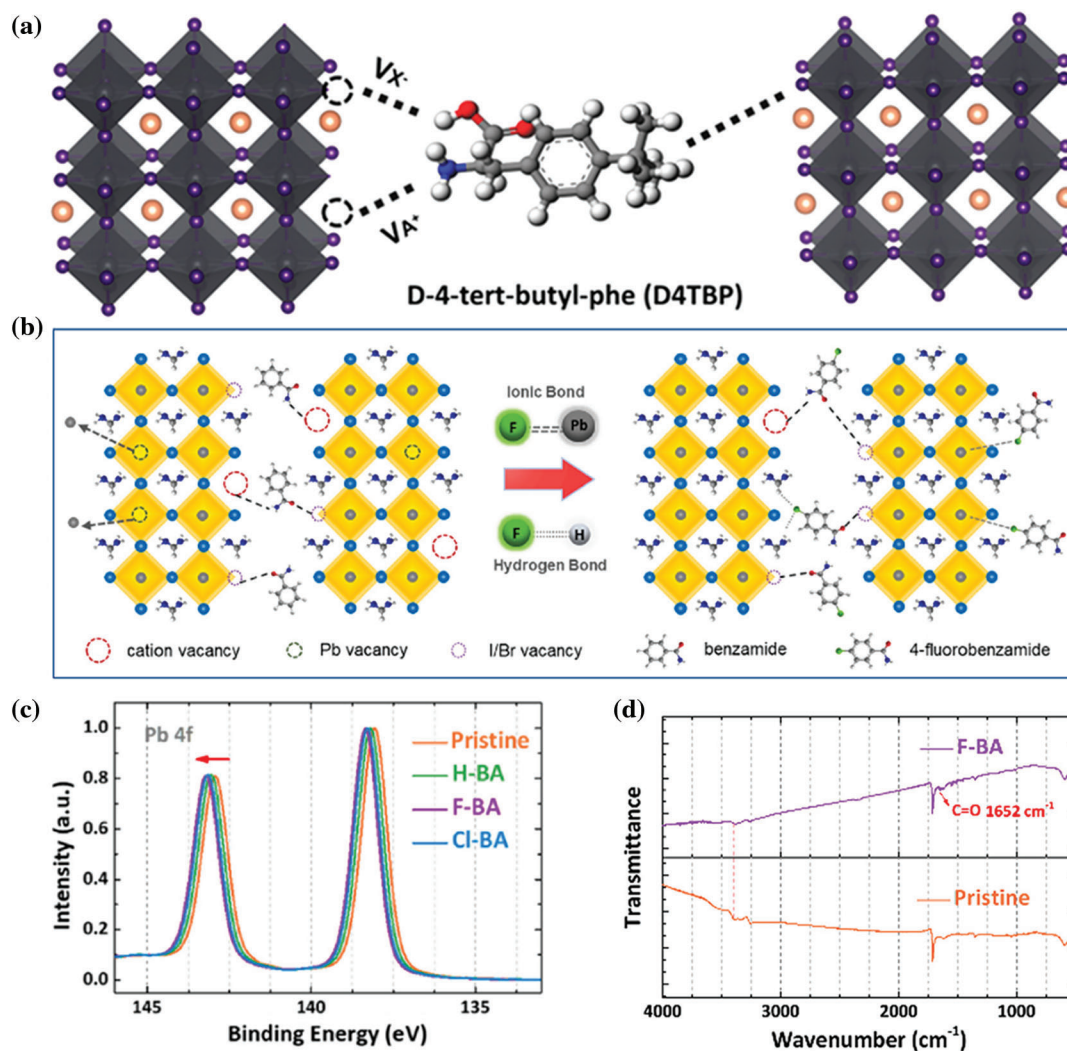
PVSCs received a  $V_{oc}$  of 1.17 V and a PCE of 20.49%. In order to study the passivation effects of molecules with different functional groups, Huang et al. designed and synthesized the D-4-tert-butylphenylalanine (D4TBP) molecule, which contains amino group, carboxyl group and benzene ring [113]. The results revealed that carboxyl and amine groups can heal charged defects through static electricity interaction, while neutral iodine-related defects can be passivated by the aromatic structure (Fig. 7a). The defect passivation reduces the  $V_{oc}$  deficit to 0.34 V and boosts the efficiency to 21.4%.



**Figure 6:** (a) Ultraviolet-visible absorption spectroscopy of the PCBM in hybrid solution and normal solution [104]. Reproduced with permission. Copyright 2015, Nature Communications. (b) Steady-state PL spectra of perovskite in the presence of the C<sub>60</sub>, PC<sub>61</sub>BM and IC<sub>60</sub>BA [107]. Reproduced with permission. Copyright 2015, Advanced Energy Materials. (c) Schematic view of the halogen bond interaction between the iodopentafluorobenzene (IPFB, halogen bond donor) and a generic halogen anion ( $X^- = I^-, Br^-, Cl^-$ , halogen bond acceptor) with  $sp^3$ -hybridized valence electrons. Schematic view of the IPFB assembly on the crystal surface [108]. Reproduced with permission. Copyright 2014, Nano Letters

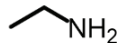
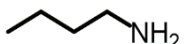
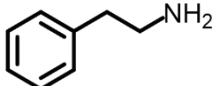
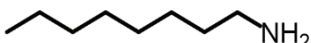
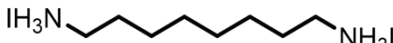

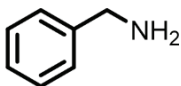
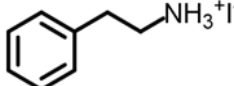
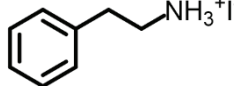
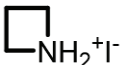
Designing effective passivation molecules has become an important method of inhibiting charge recombination and reducing voltage loss of PVSCs. A good surface passivation molecule should both passivating negative/positive and neutral defect, Liu et al. [114] customized multifunctional passivation molecules benzamide (H-BA), 4-fluorobenzamide (F-BA) and 4-chlorobenzamide (Cl-BA) by varying halogen functional groups. According to Fig. 7b, the organic cation vacancies and iodine vacancies can be partially passivated by H-BA molecule. After introducing halogen functional groups, the Pb<sup>2+</sup> and FA<sup>+</sup> can be anchored due to strong bonding. The formed ionic bonds can be verified by XPS spectra of Pb 4f

(Fig. 7c). Compared with the control film, the  $\text{Pb}^{2+}$  4f orbital has shifted to a relatively higher energy, indicating a stronger bonding. While for the FT-IR measurements (Fig. 7d), the shift of the N-H vibration ( $3500\text{--}3350\text{ cm}^{-1}$ ) of F-BA support the formation of hydrogen bonds ( $\text{N-H}\cdots\text{F}$ ). Table 1 summarizes the passivation molecular, device structure and PCEs of the discussed in this paper.

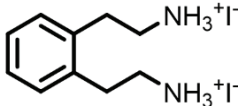
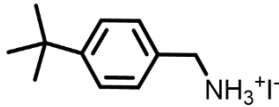
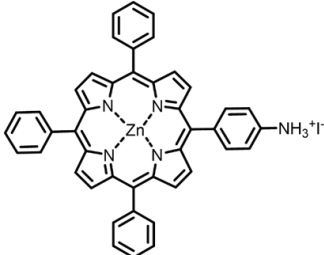
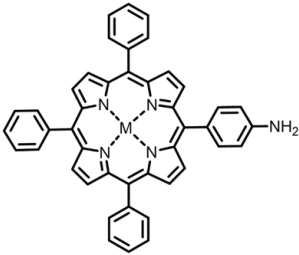
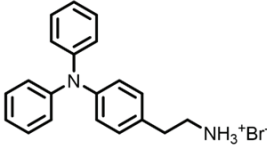
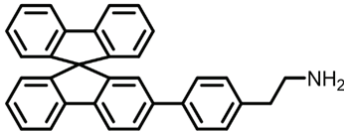


**Figure 7:** (a) Schematic illustration of the origin of D4TBP passivation effect on different defect sites [113]. Reproduced with permission. Copyright 2019, Journal of the American Chemical Society. (b) Schematic illustration for multifunctional passivation on different defect sites and ion migrations [114]. (c) XPS spectra of Pb 4f for pristine, H-BA, F-BA and Cl-BA films [114]. (d) FT-IR spectra of F-BA and pristine perovskites [114]. Reproduced with permission. Copyright 2021, Chemical Engineering Journal


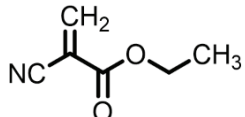
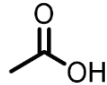
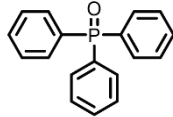
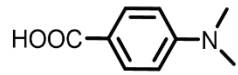
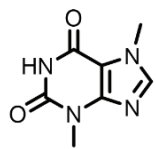
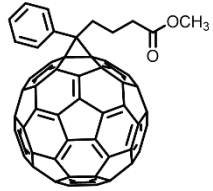

**Table 1:** Summary of passivation molecular

Passivator	Perovskite	PCE	Ref.
 Ethylamine (EA)	$\text{FA}_{0.9}\text{Cs}_{0.07}\text{MA}_{0.03}\text{Pb}(\text{I}_{0.92}\text{Br}_{0.08})_3$	22.3%	[80]
 n-Butylamine (BA)	$\text{FA}_{0.83}\text{Cs}_{0.17}\text{Pb}(\text{I}_y\text{Br}_{1-y})_3$	17.5%	[81]
 Phenethylamine (PEA)	$\text{FAPbI}_3$	13.30%	[82]
 Octylamine (OA)	$\text{MAPbI}_3$	20.10%	[83]
 Di-octylamine iodide ( $\text{C}_8$ )	$\text{MAPbI}_3$	17.60%	[84]
 n-Butylamine hydroiodate (BAI)	$\text{MAPbI}_3$	19.56%	[85]
 Benzylamine (BnA)	$\text{FAPbI}_3$	19.20%	[87]
 Phenethylamine hydroiodate (PEAI)	$\text{FAPbI}_3$	16.84%	[88]
 Phenethylamine hydroiodate (PEAI)	$(\text{FAPbI}_3)_{0.92}(\text{MAPbBr}_3)_{0.08}$	23.32%	[8]
 Azetidinium iodide (AzI)	$\text{Cs}_{0.05}\text{MA}_{0.1}\text{FA}_{0.85}\text{PbI}_{2.7}\text{Br}_{0.3}$	22.4%	[89]
	$(\text{FAPbI}_3)_{0.8}(\text{MAPbBr}_3)_{0.2}$	23.90%	[91]

(Continued)

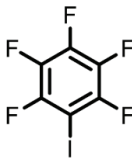
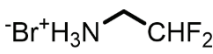
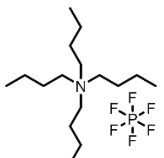
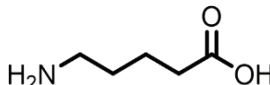
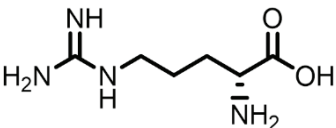
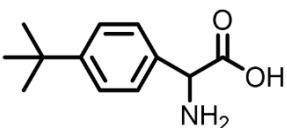
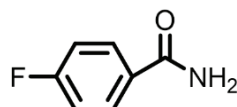
Table 1 (continued)			
Passivator	Perovskite	PCE	Ref.
 <p>o-(phenylene)di(ethylammonium) iodide (PDEAI<sub>2</sub>)</p>			
 <p>4-tert-butyl-benzylammonium iodide (tBBAI)</p>	Cs <sub>0.05</sub> FA <sub>0.85</sub> MA <sub>0.10</sub> Pb(I <sub>0.97</sub> Br <sub>0.03</sub> ) <sub>3</sub>	23.50%	[92]
 <p>Zinc porphyrin (ZnP)</p>	MAPbI <sub>3</sub>	20.5%	[93]
 <p>Porphyrins (MPs M: Co, Ni, Cu, Zn, H)</p>	Cs <sub>0.05</sub> Rb <sub>0.05</sub> (FA <sub>0.83</sub> MA <sub>0.17</sub> ) <sub>0.90</sub> Pb(I <sub>0.95</sub> Br <sub>0.05</sub> ) <sub>3</sub>	24.16%	[94]
 <p>N-((4-(N,N,N-triphenyl)phenyl) ethyl)ammonium bromide (TPA- PEABr)</p>	(FAPbI <sub>3</sub> ) <sub>0.97</sub> (MAPbBr <sub>3</sub> ) <sub>0.03</sub>	18.15%	[95]
 <p>2-(4-ethylaminobenzene)-9,9'- spirobifluorene (BSBF-NH<sub>2</sub>)</p>	(FAPbI <sub>3</sub> ) <sub>0.97</sub> (MAPbBr <sub>3</sub> ) <sub>0.03</sub>	20.05%	[96]

(Continued)

Table 1 (continued)			
Passivator	Perovskite	PCE	Ref.
 Thiophene	$\text{CH}_3\text{NH}_3\text{PbI}_{3-x}\text{Cl}_x$	16.5%	[98]
Pyridine 	$\text{MAPbI}_3$	21.03%	[99]
2-cyanoacrylate (E2CA) 	$\text{Cs}_{0.05}\text{FA}_{0.90}\text{MA}_{0.05}\text{Pb}(\text{I}_{0.95}\text{Br}_{0.05})_3$	19.20%	[100]
Acetic acid (Ac) 	$(\text{FAPbI}_3)_x(\text{MAPbBr}_3)_{1-x}$	22.10%	[101]
tribenzylphosphine oxide (TBPO) 	$\text{MAPbI}_3$	19.87%	[102]
4-dimethylaminobenzoic acid (4-DMABA) 	$(\text{FAPbI}_3)_x(\text{MAPbBr}_3)_{1-x}$	22.60%	[103]
Theophylline 	$\text{MAPbI}_3$	14.40%	[104]
PCBM 	$\text{MAPbI}_3$	15.4%	[107]
Fullerene ( $\text{C}_{60}$ )			

(Continued)



Table 1 (continued)			
Passivator	Perovskite	PCE	Ref.
 Iodopentafluorobenzene (IPFB)	MAPbI <sub>3</sub>	15.7%	[108]
 Formamidinium bromide (FABr)	MAPbI <sub>3</sub>	21.60%	[109]
 Tetrabutylammonium hexafluorophosphate (TBAPF6)	MAPbI <sub>3</sub>	21.23%	[110]
 Aminovaleric acid (AVA)	MAPbI <sub>3</sub>	9.1%	[111]
 Amino acids (NAAs)	MAPbI <sub>3</sub>	20.49%	[112]
 D-4-tert-butylphenylalanine (D4TBP)	Cs <sub>0.05</sub> FA <sub>0.81</sub> MA <sub>0.14</sub> PbI <sub>2.55</sub> Br <sub>0.45</sub>	21.40%	[113]
 4-fluorobenzamide (F-BA)	Cs <sub>0.025</sub> FA <sub>0.825</sub> MA <sub>0.15</sub> Pb(I <sub>0.85</sub> Br <sub>0.15</sub> ) <sub>3</sub>	21.35%	[114]

#### 4 Conclusion and Outlook

The performance improvement of PVSCs is significant, achieving high efficiency comparable to silicon cells in less than ten years. However, the current PCE is not enough, and the long-term stability should be improved thus guaranteeing its market entrance. Passivation at the grain boundaries and interfaces can increase the grain size of the perovskite film, promote the formation of pure phases, reduce surface pores,

and form a smooth and dense perovskite layer. It is an effective means to further improve the PCE of PVSCs. In addition, the introduction of passivating molecules in the interface can reduce the formation of interface defects and the recombination of carriers, extend the diffusion distance of carriers, and facilitate the transport of carriers at the interface.

In this review, we summarize the research and results of organic molecules as passivators to improve the photovoltaic performance of PVSCs. Focus has been given to the influence of functional groups on defect passivation and device performance. These results indicate that organic passivation molecules can make an important contribution to the further development of high-efficiency perovskite solar cells. Compared with the single passivation effect of traditional organic molecules, multifunctional passivation molecules can improve the PCE of PVSCs in many ways.

Although great progress has been made in the interface engineering for efficient and stable PVSCs, there is still a big gap in commercial applications. In general, the wide application of PVSCs has potential difficulties and challenges, that is, the manufacturing process of large-area nanomaterials, long-term stability, device encapsulation technology, and the toxicity of perovskite films. In order to accelerate the commercialization of PVSCs, it is necessary to actively explore good interface modification methods and develop excellent interface modification materials suitable for PVSCs. These strategies will lay a solid foundation for the long-term stability of PVSCs and the development towards industrialization.

**Funding Statement:** Financial support from Key Program of National Natural Science Foundation of China (22133006), the National Natural Science Foundation of China (ZX20210286), the Fundamental Research Funds for the Central Universities (20CX06004A), Talent Introduction Program of China University of Petroleum (East China) (ZX20190162) and the Post-Graduate Innovation Project of China University of Petroleum (East China) (YCX2021140) are acknowledged. We also thank the support from the Yankuang Group 2019 Science and Technology Program (YKKJ2019AJ05JG-R60). Prof. X. Li and Dr. T. Zhang thank the Taishan Scholar Program of Shandong Province (ts201712019, tsnq201909069) for financial support.

**Conflicts of Interest:** The authors declare that they have no conflicts of interest to report regarding the present study.

## References

1. Kojima, A., Teshima, K., Shirai, Y., Miyasaka, T. (2009). Organometal halide perovskites as visible-light sensitizers for photovoltaic cells. *Journal of the American Chemical*, 131(17), 6050–6051. DOI 10.1021/ja809598r.
2. Best Research-Cell Efficiency Chart (2022). <https://www.nrel.gov/pv/cellefficiency.html>.
3. Stranks, S. D., Eperon, G. E., Grancini, G., Menelaou, C., Alcocer, M. J. et al. (2013). Electron-hole diffusion lengths exceeding 1 micrometer in an organometal trihalide perovskite absorber. *Science*, 342(6156), 341–344. DOI 10.1126/science.1243982.
4. Shi, D., Adinolfi, V., Comin, R., Yuan, M., Alarousu, E. et al. (2015). Low trap-state density and long carrier diffusion in organolead trihalide perovskite single crystals. *Science*, 347(6221), 519–522. DOI 10.1126/science.aaa2725.
5. Lu, H., Liu, Y., Ahlawat, P., Mishra, A., Tress, W. R. et al. (2020). Vapor-assisted deposition of highly efficient, stable black-phase FAPbI<sub>3</sub> perovskite solar cells. *Science*, 370(6512), 8985. DOI 10.1126/science.abb8985.
6. Vasilopoulou, M., Fakharuddin, A., Coutsolelos, A. G., Falaras, P., Argitis, P. et al. (2020). Molecular materials as interfacial layers and additives in perovskite solar cells. *Chemical Society Reviews*, 49(13), 4496–4526. DOI 10.1039/C9CS00733D.
7. Luo, D., Su, R., Zhang, W., Gong, Q., Zhu, R. (2020). Minimizing non-radiative recombination losses in perovskite solar cells. *Nature Reviews Materials*, 5(1), 44–60. DOI 10.1038/s41578-019-0151-y.
8. Jiang, Q., Zhao, Y., Zhang, X., Yang, X., Chen, Y. et al. (2019). Surface passivation of perovskite film for efficient solar cells. *Nature Photonics*, 13(7), 460–466. DOI 10.1038/s41566-019-0398-2.

9. Zheng, X., Chen, B., Dai, J., Fang, Y., Bai, Y. et al. (2017). Defect passivation in hybrid perovskite solar cells using quaternary ammonium halide anions and cations. *Nature Energy*, 2(7), 17102. DOI 10.1038/nenergy.2017.102.
10. Zohar, A., Kulbak, M., Levine, I., Hodes, G., Kahn, A. et al. (2018). What limits the open-circuit voltage of bromide perovskite-based solar cells? *ACS Energy Letters*, 4(1), 1–7. DOI 10.1021/acsenenergylett.8b01920.
11. Chen, Q., Zhou, H., Song, T. B., Luo, S., Hong, Z. et al. (2014). Controllable self-induced passivation of hybrid lead iodide perovskites toward high performance solar cells. *Nano Letters*, 14(7), 4158–4163. DOI 10.1021/nl501838y.
12. Wang, K., Wu, C., Hou, Y., Yang, D., Ye, T. et al. (2020). Isothermally crystallized perovskites at room-temperature. *Energy & Environmental Science*, 13(10), 3412–3422. DOI 10.1039/D0EE01967D.
13. Li, B., Zhang, Q., Zhang, S., Ahmad, Z., Chidanguro, T. et al. (2021). Spontaneously supersaturated nucleation strategy for high reproducible and efficient perovskite solar cells. *Chemical Engineering Journal*, 405, 126998. DOI 10.1016/j.cej.2020.126998.
14. Yi, M., Shen, Z., Zhao, X., Liang, S., Liu, L. (2014). Boron nitride nanosheets as oxygen-atom corrosion protective coatings. *Applied Physics Letters*, 104(14), 143101. DOI 10.1063/1.4870530.
15. Kim, J., Lee, S. H., Lee, J. H., Hong, K. H. (2014). The role of intrinsic defects in methylammonium lead iodide perovskite. *The Journal of Physical Chemistry Letters*, 5(8), 1312–1317. DOI 10.1021/jz500370k.
16. Shao, Y., Xiao, Z., Bi, C., Yuan, Y., Huang, J. (2014). Origin and elimination of photocurrent hysteresis by fullerene passivation in  $\text{CH}_3\text{NH}_3\text{PbI}_3$  planar heterojunction solar cells. *Nature Communications*, 5(1), 5784. DOI 10.1038/ncomms6784.
17. Chen, Q., Chen, J., Yang, Z., Xu, J., Xu, L. et al. (2019). Nanoparticle-enhanced radiotherapy to trigger robust cancer immunotherapy. *Advanced Materials*, 31(10), 1802228. DOI 10.1002/adma.201802228.
18. Wu, N., Wu, Y., Walter, D., Shen, H., Duong, T. et al. (2017). Identifying the cause of voltage and fill factor losses in perovskite solar cells by using luminescence measurements. *Energy Technology*, 5(10), 1827–1835. DOI 10.1002/ente.201700374.
19. Zhu, T. Y., Shu, D. J. (2021). Polarization-controlled surface defect formation in a hybrid Perovskite. *The Journal of Physical Chemistry Letters*, 12(16), 3898–3906. DOI 10.1021/acs.jpcclett.1c00702.
20. Zhao, L., Rand, B. P. (2021). Alleviating halide perovskite surface defects. *Matter*, 4(7), 2104–2105. DOI 10.1016/j.matt.2021.06.008.
21. Qi, W., Zhou, X., Li, J., Cheng, J., Li, Y. et al. (2020). Inorganic material passivation of defects toward efficient perovskite solar cells. *Science Bulletin*, 65(23), 2022–2032. DOI 10.1016/j.scib.2020.07.017.
22. Bu, T., Li, J., Zheng, F., Chen, W., Wen, X. et al. (2018). Universal passivation strategy to slot-die printed  $\text{SnO}_2$  for hysteresis-free efficient flexible perovskite solar module. *Nature Communications*, 9(1), 1–10. DOI 10.1038/s41467-018-07099-9.
23. Chen, C., Xu, Y., Wu, S., Zhang, S., Yang, Z. et al. (2018).  $\text{CaI}_2$ : A more effective passivator of perovskite films than  $\text{PbI}_2$  for high efficiency and long-term stability of perovskite solar cells. *Journal of Materials Chemistry A*, 6(17), 7903–7912. DOI 10.1039/C7TA11280G.
24. Han, S., Zhang, H., Wang, R., He, Q. (2021). Research progress of absorber film of inorganic perovskite solar cells: Fabrication techniques and additive engineering in defect passivation. *Materials Science in Semiconductor Processing*, 127(6196), 105666. DOI 10.1016/j.mssp.2021.105666.
25. Li, R., Dou, Y., Liao, Y., Wang, D., Li, G. et al. (2022). Enhancing efficiency of perovskite solar cells from surface passivation of  $\text{Co}^{2+}$  doped  $\text{CuGaO}_2$  nanocrystals. *Journal of Colloid and Interface Science*, 607(1), 1280–1286. DOI 10.1016/j.jcis.2021.09.102.
26. Choi, H., Liu, X., Kim, H. I., Kim, D., Park, T. et al. (2021). A facile surface passivation enables thermally stable and efficient planar perovskite solar cells using a novel IDTT-based small molecule additive. *Advanced Energy Materials*, 11(16), 2003829. DOI 10.1002/aenm.202003829.
27. Jeong, M., Choi, I. W., Go, E. M., Cho, Y., Kim, M. et al. (2020). Stable perovskite solar cells with efficiency exceeding 24.8% and 0.3 V voltage loss. *Science*, 369(6511), 1615–1620. DOI 10.1126/science.abb7167.

28. Yang, J., Tang, W., Yuan, R., Chen, Y., Wang, J. et al. (2021). Defect mitigation using D-penicillamine for efficient methylammonium-free perovskite solar cells with high operational stability. *Chemical Science*, 12, 2050–2059. DOI 10.1039/D0SC06354A.
29. Aktas, E., Jiménez-López, J., Rodríguez-Seco, C., Pudi, R., Ortuño, M. A. et al. (2019). Supramolecular coordination of  $\text{Pb}^{2+}$  defects in hybrid lead halide perovskite films using truxene derivatives as Lewis base interlayers. *ChemPhysChem*, 20(20), 2702–2711. DOI 10.1002/cphc.201900068.
30. Sun, Y., Zhang, J., Yu, H., Huang, C., Huang, J. (2022). Several triazine-based small molecules assisted in the preparation of high-performance and stable perovskite solar cells by trap passivation and heterojunction engineering. *ACS Applied Materials & Interfaces*, 14(5), 6625–6637. DOI 10.1021/acsami.1c21081.
31. Song, Q., Gong, H., Ji, C., Zhang, H., Sun, F. et al. (2021). Perovskite passivation with a bifunctional molecule 1,2-benzisothiazolin-3-one for efficient and stable planar solar cells. *Solar RRL*, 5(10), 2100472. DOI 10.1002/solr.202100472.
32. Han, F., Hao, G., Wan, Z., Luo, J., Xia, J. et al. (2018). Bifunctional electron transporting layer/perovskite interface linker for highly efficient perovskite solar cells. *Electrochimica Acta*, 296, 75–81. DOI 10.1016/j.electacta.2018.10.130.
33. Liu, G., Liu, C., Lin, Z., Yang, J., Huang, Z. et al. (2020). Regulated crystallization of efficient and stable tin-based perovskite solar cells via a self-sealing polymer. *ACS Applied Materials & Interfaces*, 12(12), 14049–14056. DOI 10.1021/acsami.0c01311.
34. Yang, Q., Wang, X., Yu, S., Liu, X., Gao, P. et al. (2021). Solvent-actuated self-assembly of amphiphilic hole-transporting polymer enables bottom-surface passivation of perovskite film for efficient photovoltaics. *Advanced Energy Materials*, 11(17), 2100493. DOI 10.1002/aenm.202100493.
35. Li, F., Yuan, J., Ling, X., Zhang, Y., Yang, Y. et al. (2018). A universal strategy to utilize polymeric semiconductors for perovskite solar cells with enhanced efficiency and longevity. *Advanced Functional Materials*, 28(15), 1706377. DOI 10.1002/adfm.201706377.
36. Wu, T., Li, X., Qi, Y., Zhang, Y., Han, L. (2021). Defect passivation for perovskite solar cells: From molecule design to device performance. *ChemSusChem*, 14(20), 4354–4376. DOI 10.1002/cssc.202101573.
37. Ni, Z., Bao, C., Liu, Y., Jiang, Q., Wu, W. Q. et al. (2020). Resolving spatial and energetic distributions of trap states in metal halide perovskite solar cells. *Science*, 367(6484), 1352–1358. DOI 10.1126/science.aba0893.
38. Wen, L., Rao, Y., Zhu, M., Li, R., Zhan, J. et al. (2021). Reducing defects density and enhancing hole extraction for efficient perovskite solar cells enabled by  $\pi\text{-Pb}^{2+}$  interactions. *Angewandte Chemie International Edition*, 60(32), 17356–17361. DOI 10.1002/anie.202102096.
39. Heo, S., Seo, G., Lee, Y., Lee, D., Seol, M. et al. (2017). Deep level trapped defect analysis in  $\text{CH}_3\text{NH}_3\text{PbI}_3$  perovskite solar cells by deep level transient spectroscopy. *Energy & Environmental Science*, 10(5), 1128–1133. DOI 10.1039/c7ee00303j.
40. Duan, H. S., Zhou, H. P., Chen, Q., Sun, P. Y., Luo, S. et al. (2015). The identification and characterization of defect states in hybrid organic-inorganic perovskite photovoltaics. *Physical Chemistry Chemical Physics*, 17(1), 112–116. DOI 10.1039/c4cp04479g.
41. Hutter, E. M., Eperon, G. E., Stranks, S. D., Savenije, T. J. (2015). Charge carriers in planar and meso-structured organic-inorganic perovskites: Mobilities, lifetimes, and concentrations of trap states. *The Journal of Physical Chemistry Letters*, 6(15), 3082–3090. DOI 10.1021/acs.jpclett.5b01361.
42. Yang, X., Ni, Y., Zhang, Y., Wang, Y., Yang, W. et al. (2021). Multiple-defect management for efficient perovskite photovoltaics. *ACS Energy Letters*, 6(7), 2404–2412. DOI 10.1021/acsenergylett.1c01039.
43. Yuan, Y., Huang, J. (2016). Ion migration in organometal trihalide perovskite and its impact on photovoltaic efficiency and stability. *Accounts of Chemical Research*, 49(2), 286–293. DOI 10.1021/acs.accounts.5b00420.
44. Chen, Y., Zhou, H. (2020). Defects chemistry in high-efficiency and stable perovskite solar cells. *Journal of Applied Physics*, 128(6), 60903. DOI 10.1063/5.0012384.
45. Yin, W. J., Shi, T., Yan, Y. (2014). Unusual defect physics in  $\text{CH}_3\text{NH}_3\text{PbI}_3$  perovskite solar cell absorber. *Applied Physics Letters*, 104(6), 63903. DOI 10.1063/1.4864778.

46. Wang, Q., Shao, Y., Xie, H., Lyu, L., Liu, X. et al. (2014). Qualifying composition dependent p and n self-doping in  $\text{CH}_3\text{NH}_3\text{PbI}_3$ . *Applied Physics Letters*, 105(16), 163508. DOI 10.1063/1.4899051.
47. Xing, G., Mathews, N., Sun, S., Lim, S. S., Lam, Y. M. et al. (2013). Long-range balanced electron and hole-transport lengths in organic-inorganic  $\text{CH}_3\text{NH}_3\text{PbI}_3$ . *Science*, 342(6156), 344–347. DOI 10.1126/science.1243167.
48. Shi, T., Yin, W., Feng, H., Kai, Z., Yan, Y. (2015). Unipolar self-doping behavior in perovskite  $\text{CH}_3\text{NH}_3\text{PbBr}_3$ . *Applied Physics Letters*, 106(10), 6050–6051. DOI 10.1063/1.4914544.
49. Agiorgousis, M. L., Sun, Y. Y., Zeng, H., Zhang, S. (2014). Strong Covalency-induced recombination centers in perovskite solar cell material  $\text{CH}_3\text{NH}_3\text{PbI}_3$ . *Journal of the American Chemical Society*, 136(41), 14570–14575. DOI 10.1021/ja5079305.
50. Taufique, M. F. N., Khanal, R., Choudhury, S., Banerjee, S. (2018). Impact of iodine antisite (IPb) defects on the electronic properties of the (110)  $\text{CH}_3\text{NH}_3\text{PbI}_3$  surface. *The Journal of Chemical Physics*, 149(16), 164704. DOI 10.1063/1.5044667.
51. Bi, D. Q., El-Zohry, A. M., Hagfeldt, A., Boschloo, G. (2014). Improved morphology control using a modified two-step method for efficient perovskite solar cells. *ACS Applied Materials & Interfaces*, 6(21), 18751–18757. DOI 10.1021/am504320h.
52. Uratani, H., Yamashita, K. (2017). Charge carrier trapping at surface defects of perovskite solar cell absorbers: A first-principles study. *Journal of Physical Chemistry Letters*, 8(4), 742–746. DOI 10.1021/acs.jpclett.7b00055.
53. Patel, J. B., Milot, R. L., Wright, A. D., Herz, L. M., Johnston, M. B. (2016). Formation dynamics of  $\text{CH}_3\text{NH}_3\text{PbI}_3$  perovskite following two-step layer deposition. *Journal of Physical Chemistry Letters*, 7(1), 96–102. DOI 10.1021/acs.jpclett.5b02495.
54. Xiao, Z., Yuan, Y., Wang, Q., Shao, Y., Bai, Y. et al. (2016). Thin-film semiconductor perspective of organometal trihalide perovskite materials for high-efficiency solar cells. *Materials Science and Engineering: R: Reports*, 101, 1–38. DOI 10.1016/j.mser.2015.12.002.
55. Fu, L., Li, H., Wang, L., Yin, R. Y., Li, B. et al. (2020). Defect passivation strategies in perovskites for an enhanced photovoltaic performance. *Energy & Environmental Science*, 13(11), 4017–4056. DOI 10.1039/d0ee01767a.
56. Srivastava, V., Alexander, A., Anitha, B., Namboothiry, M. A. G. (2022). Impedance spectroscopy study of defect/ion mediated electric field and its effect on the photovoltaic performance of perovskite solar cells based on different active layers. *Solar Energy Materials and Solar Cells*, 237, 111548. DOI 10.1016/j.solmat.2021.111548.
57. Bi, E., Song, Z., Li, C., Wu, Z., Yan, Y. (2021). Mitigating ion migration in perovskite solar cells. *Trends in Chemistry*, 3(7), 575–588. DOI 10.1016/j.trechm.2021.04.004.
58. Li, Z., Xiao, C., Yang, Y., Harvey, S. P., Kim, D. H. et al. (2017). Extrinsic ion migration in perovskite solar cells. *Energy & Environmental Science*, 10(5), 1234–1242. DOI 10.1039/C7EE00358G.
59. Azpiroz, J. M., Mosconi, E., Bisquert, J., de Angelis, F. (2015). Defect migration in methylammonium lead iodide and its role in perovskite solar cell operation. *Energy & Environmental Science*, 8(7), 2118–2127. DOI 10.1039/C5EE01265A.
60. Yuan, Y., Li, T., Wang, Q., Xing, J., Gruverman, A. et al. (2017). Anomalous photovoltaic effect in organic-inorganic hybrid perovskite solar cells. *Science Advances*, 3(3), e1602164. DOI 10.1126/sciadv.1602164.
61. Li, C., Tscheuschner, S., Paulus, F., Hopkinson, P. E., Kießling, J. et al. (2016). Iodine migration and its effect on hysteresis in perovskite solar cells. *Advanced Materials*, 28(12), 2446–2454. DOI 10.1002/adma.201503832.
62. Roose, B. (2021). Ion migration drives self-passivation in perovskite solar cells and is enhanced by light soaking. *RSC Advances*, 11(20), 12095–12101. DOI 10.1039/D1RA01166A.
63. Xing, J., Wang, Q., Dong, Q., Yuan, Y., Fang, Y. et al. (2016). Ultrafast ion migration in hybrid perovskite polycrystalline thin films under light and suppression in single crystals. *Physical Chemistry Chemical Physics*, 18(44), 30484–30490. DOI 10.1039/C6CP06496E.
64. de Quilettes, D. W., Vorpahl, S. M., Stranks, S. D., Nagaoka, H., Eperon, G. E. et al. (2015). Impact of microstructure on local carrier lifetime in perovskite solar cells. *Science*, 348(6235), 683–686. DOI 10.1126/science.aaa5333.



65. Ball, J. M., Petrozza, A. (2016). Defects in perovskite-halides and their effects in solar cells. *Nature Energy*, 1, 16149. DOI 10.1038/nenergy.2016.149.
66. Zhao, Y. C., Zhou, W. K., Zhou, X., Liu, K. H., Yu, D. P. et al. (2017). Quantification of light-enhanced ionic transport in lead iodide perovskite thin films and its solar cell applications. *Light: Science & Applications*, 6(5), e16243. DOI 10.1038/lsa.2016.243.
67. Frost, J. M., Butler, K. T., Brivio, F., Hendon, C. H., van Schilfgaarde, M. et al. (2014). Atomistic origins of high-performance in hybrid halide perovskite solar cells. *Nano Letters*, 14(5), 2584–2590. DOI 10.1021/nl500390f.
68. Aristidou, N., Sanchez-Molina, I., Chotchuangchutchaval, T., Brown, M., Martinez, L. et al. (2015). The role of oxygen in the degradation of methylammonium lead trihalide perovskite photoactive layers. *Angewandte Chemie*, 127(28), 8326–8330. DOI 10.1002/ange.201503153.
69. Ouyang, Y., Shi, L., Li, Q., Wang, J. (2019). Role of water and defects in photo-oxidative degradation of methylammonium lead iodide perovskite. *Small Methods*, 1900154. DOI 10.1002/smt.201900154.
70. Zong, Y., Zhou, Z., Chen, M., Padture, N. P., Zhou, Y. (2018). Lewis-adduct mediated grain-boundary functionalization for efficient ideal-bandgap perovskite solar cells with superior stability. *Advanced Energy Materials*, 8(27), 1800997. DOI 10.1002/aenm.201800997.
71. Wang, C., Song, Z., Zhao, D., Awni, R. A., Li, C. et al. (2019). Improving performance and stability of planar perovskite solar cells through grain boundary passivation with block copolymers. *Solar RRL*, 3(9), 1900078. DOI 10.1002/solr.201900078.
72. Wang, Q., Chen, B., Liu, Y., Deng, Y., Bai, Y. et al. (2017). Scaling behavior of moisture-induced grain degradation in polycrystalline hybrid perovskite thin films. *Energy & Environmental Science*, 10(2), 516–522. DOI 10.1039/C6EE02941H.
73. Ahn, N., Kwak, K., Jang, M. S., Yoon, H., Lee, B. Y. et al. (2016). Trapped charge-driven degradation of perovskite solar cells. *Nature Communications*, 7(1), 13422. DOI 10.1038/ncomms13422.
74. Aristidou, N., Eames, C., Sanchez-Molina, I., Bu, X., Kosco, J. et al. (2017). Fast oxygen diffusion and iodide defects mediate oxygen-induced degradation of perovskite solar cells. *Nature Communications*, 8(1), 15218. DOI 10.1038/ncomms15218.
75. Wang, F., Bai, S., Tress, W., Hagfeldt, A., Gao, F. (2018). Defects engineering for high-performance perovskite solar cells. *npj Flexible Electronics*, 2(1), 22. DOI 10.1038/s41528-018-0035-z.
76. Mahmud, M. A., Duong, T., Yin, Y. T., Pham, H. T., Walter, D. et al. (2020). Double-sided surface passivation of 3D perovskite film for high-efficiency mixed-dimensional perovskite solar cells. *Advanced Functional Materials*, 30(7). DOI 10.1002/adfm.201907962.
77. Li, X., Sheng, W., Duan, X., Lin, Z., Yang, J. et al. (2021). Defect passivation effect of chemical groups on perovskite solar cells. *ACS Applied Materials & Interfaces*. DOI 10.1021/acsami.1c08539.
78. Zhang, W., Li, Q. S., Li, Z. S. (2021). Understanding the surface passivation effects of Lewis base in perovskite solar cells. *Applied Surface Science*, 563, 150267. DOI 10.1016/j.apsusc.2021.150267.
79. Yusoff, A., Vasilopoulou, M., Georgiadou, D. G., Palilis, L. C., Abate, A. et al. (2021). Passivation and process engineering approaches of halide perovskite films for high efficiency and stability perovskite solar cells. *Energy & Environmental Science*, 14(15), 2906–2953. DOI 10.1039/d1ee00062d.
80. Alharbi, E. A., Alyamani, A. Y., Kubicki, D. J., Uhl, A. R., Walder, B. J. et al. (2019). Atomic-level passivation mechanism of ammonium salts enabling highly efficient perovskite solar cells. *Nature Communications*, 10(1), 1–9. DOI 10.1038/s41467-019-10985-5.
81. Wang, Z. P., Lin, Q. Q., Chmiel, F. P., Sakai, N., Herz, L. M. et al. (2017). Efficient ambient-air-stable solar cells with 2D-3D heterostructured butylammonium-caesium-formamidinium lead halide perovskites. *Nature Energy*, 2(9), 17135. DOI 10.1038/nenergy.2017.135.
82. Thote, A., Jeon, I., Lee, J. W., Seo, S., Lin, H. S. et al. (2019). Stable and reproducible 2D/3D formamidinium-lead-iodide perovskite solar cells. *ACS Applied Energy Materials*, 2(4), 2486–2493. DOI 10.1021/acsaem.8b01964.

83. Jung, M., Shin, T. J., Seo, J., Kim, G., Seok, S. I. (2018). Structural features and their functions in surfactant-armoured methylammonium lead iodide perovskites for highly efficient and stable solar cells. *Energy & Environmental Science*, 11(8), 2188–2197. DOI 10.1039/C8EE00995C.
84. Zhao, T., Chueh, C. C., Chen, Q., Rajagopal, A., Jen, K. Y. (2016). Defect passivation of organic-inorganic hybrid perovskites by diammonium iodide toward high-performance photovoltaic devices. *ACS Energy Letters*, 1(4), 757–763. DOI 10.1021/acseenergylett.6b00327.
85. Lin, Y., Bai, Y., Fang, Y., Chen, Z., Yang, S. et al. (2018). Enhanced thermal stability in perovskite solar cells by assembling 2D/3D stacking structures. *The Journal of Physical Chemistry Letters*, 9(3), 654–658. DOI 10.1021/acs.jpclett.7b02679.
86. Gao, F., Zhao, Y., Zhang, X., You, J. (2020). Recent progresses on defect passivation toward efficient perovskite solar cells. *Advanced Energy Materials*, 10(13), 1902650. DOI 10.1002/aenm.201902650.
87. Wang, F., Geng, W., Zhou, Y., Fang, H. H., Tong, C. et al. (2016). Phenylalkylamine passivation of organolead halide perovskites enabling high-efficiency and air-stable photovoltaic cells. *Advanced Materials*, 28(45), 9986–9992. DOI 10.1002/adma.201603062.
88. Hu, Y., Schlipf, J., Wussler, M., Petrus, M. L., Jaegermann, W. et al. (2016). Hybrid perovskite/perovskite heterojunction solar cells. *ACS Nano*, 10(6), 5999–6007. DOI 10.1021/acsnano.6b01535.
89. Ansari, F., Shirzadi, E., Salavati-Niasari, M., LaGrange, T., Nonomura, K. et al. (2020). Passivation mechanism exploiting surface dipoles affords high-performance perovskite solar cells. *Journal of the American Chemical Society*, 142(26), 11428–11433. DOI 10.1021/jacs.0c01704.
90. Chen, A. Z., Shiu, M., Ma, J. H., Alpert, M. R., Zhang, D. et al. (2018). Origin of vertical orientation in two-dimensional metal halide perovskites and its effect on photovoltaic performance. *Nature Communications*, 9(1), 1336. DOI 10.1038/s41467-018-03757-0.
91. Liu, C., Yang, Y., Rakstys, K., Mahata, A., Franckevicius, M. et al. (2021). Tuning structural isomers of phenylenediammonium to afford efficient and stable perovskite solar cells and modules. *Nature Communications*, 12(1), 1–9. DOI 10.1038/s41467-021-26754-2.
92. Zhu, H., Liu, Y., Eickemeyer, F. T., Pan, L., Ren, D. et al. (2020). Tailored amphiphilic molecular mitigators for stable perovskite solar cells with 23.5% efficiency. *Advanced Materials*, 32(12), 1907757. DOI 10.1002/adma.201907757.
93. Li, C., Yin, J., Chen, R., Lv, X., Feng, X. et al. (2019). Monoammonium porphyrin for blade-coating stable large-area perovskite solar cells with >18% efficiency. *Journal of the American Chemical Society*, 141(15), 6345–6351. DOI 10.1021/jacs.9b01305.
94. Fang, Z., Wang, L., Mu, X., Chen, B., Xiong, Q. et al. (2021). Grain boundary engineering with self-assembled porphyrin supramolecules for highly efficient large-area perovskite photovoltaics. *Journal of the American Chemical Society*, 143(45), 18989–18996. DOI 10.1021/jacs.1c07518.
95. Zhao, B. H., Yan, X. Y., Zhang, T., Ma, X. T., Liu, C. B. et al. (2020). Introduction of multifunctional triphenylamine derivatives at the perovskite/HTL interface to promote efficiency and stability of perovskite solar cells. *ACS Applied Materials & Interfaces*, 12(8), 9300–9306. DOI 10.1021/acsami.9b21112.
96. Zhang, T., Zhao, B., Li, Z., Liu, S., Liu, C. et al. (2022). Inspired from Spiro-OMeTAD: Developing ambipolar spirobifluorene derivatives as effective passivation molecules for perovskite solar cells. *Journal of Materials Chemistry C*, 10(4), 1357–1364. DOI 10.1039/D1TC04925A.
97. Wang, S., Wang, A., Deng, X., Xie, L., Xiao, A. et al. (2020). Lewis acid/base approach for efficacious defect passivation in perovskite solar cells. *Journal of Materials Chemistry A*, 8(25), 12201–12225. DOI 10.1039/D0TA03957H.
98. Noel, N. K., Abate, A., Stranks, S. D., Parrott, E. S., Burlakov, V. M. et al. (2014). Enhanced photoluminescence and solar cell performance via Lewis base passivation of organic-inorganic lead halide perovskites. *ACS Nano*, 8(10), 9815–9821. DOI 10.1021/nn5036476.
99. Li, X., Zhang, W., Zhang, W., Wang, H. Q., Fang, J. (2019). Spontaneous grain polymerization for efficient and stable perovskite solar cells. *Nano Energy*, 58, 825–833. DOI 10.1016/j.nanoen.2019.02.009.

100. Li, Y., Shi, J., Zheng, J., Bing, J., Yuan, J. et al. (2020). Acetic acid assisted crystallization strategy for high efficiency and long-term stable perovskite solar cell. *Advanced Science*, 7(5), 1903368. DOI 10.1002/advs.201903368.
101. Li, H., Shi, J., Deng, J., Chen, Z., Li, Y. et al. (2020). Intermolecular  $\pi$ - $\pi$  conjugation self-assembly to stabilize surface passivation of highly efficient perovskite solar cells. *Advanced Materials*, 32(23), 1907396. DOI 10.1002/adma.201907396.
102. Zhu, H., Huang, B., Wu, S., Xiong, Z., Li, J. et al. (2018). Facile surface modification of  $\text{CH}_3\text{NH}_3\text{PbI}_3$  films leading to simultaneously improved efficiency and stability of inverted perovskite solar cells. *Journal of Materials Chemistry A*, 6(15), 6255–6264. DOI 10.1039/C8TA00267C.
103. Wang, R., Xue, J., Wang, K. L., Wang, Z. K., Luo, Y. et al. (2019). Constructive molecular configurations for surface-defect passivation of perovskite photovoltaics. *Science*, 366(6472), 1509–1513. DOI 10.1126/science.aay9698.
104. Xu, J., Buin, A., Ip, A. H., Li, W., Voznyy, O. et al. (2015). Perovskite-fullerene hybrid materials suppress hysteresis in planar diodes. *Nature Communications*, 6(1), 1–8. DOI 10.1038/ncomms8081.
105. Lin, Y., Chen, B., Zhao, F., Zheng, X., Deng, Y. et al. (2017). Matching charge extraction contact for wide-bandgap perovskite solar cells. *Advanced Materials*, 29, 1700607. DOI 10.1002/adma.201700607.
106. Fang, X., Ding, J., Yuan, N., Sun, P., Lv, M. et al. (2017). Graphene quantum dot incorporated perovskite films: passivating grain boundaries and facilitating electron extraction. *Physical Chemistry Chemical Physics*, 19(8), 6057–6063. DOI 10.1039/C6CP06953C.
107. Liang, P. W., Chueh, C. C., Williams, S. T., Jen, A. K. Y. (2015). Roles of fullerene-based interlayers in enhancing the performance of organometal perovskite thin-film solar cells. *Advanced Energy Materials*, 5(10), 1402321. DOI 10.1002/aenm.201402321.
108. Abate, A., Saliba, M., Hollman, D. J., Stranks, S. D., Wojciechowski, K. et al. (2014). Supramolecular halogen bond passivation of organic-inorganic halide perovskite solar cells. *Nano Letters*, 14(6), 3247–3254. DOI 10.1021/nl500627x.
109. Dong, W., Qiao, W., Xiong, S., Yang, J., Wang, X. et al. (2022). Surface passivation and energetic modification suppress nonradiative recombination in perovskite solar cells. *Nano-Micro Letters*, 14(1), 1–11. DOI 10.1007/s40820-022-00854-0.
110. Xiong, S., Dai, Y., Yang, J., Xiao, W., Li, D. et al. (2021). Surface charge-transfer doping for highly efficient perovskite solar cells. *Nano Energy*, 79, 105505. DOI 10.1016/j.nanoen.2020.105505.
111. Lin, C. T., de Rossi, F., Kim, J., Baker, J., Ngiam, J. et al. (2019). Evidence for surface defect passivation as the origin of the remarkable photostability of unencapsulated perovskite solar cells employing aminovaleric acid as a processing additive. *Journal of Materials Chemistry A*, 7(7), 3006–3011. DOI 10.1039/C8TA11985F.
112. Hu, J., Xu, X., Chen, Y., Wu, S., Wang, Z. et al. (2021). Overcoming photovoltage deficit via natural amino acid passivation for efficient perovskite solar cells and modules. *Journal of Materials Chemistry A*, 9(9), 5857–5865. DOI 10.1039/D0TA12342K.
113. Yang, S., Dai, J., Yu, Z., Shao, Y., Zhou, Y. et al. (2019). Tailoring passivation molecular structures for extremely small open-circuit voltage loss in perovskite solar cells. *Journal of the American Chemical Society*, 141(14), 5781–5787. DOI 10.1021/jacs.8b13091.
114. Liu, G., Zheng, H., Zhang, L., Xu, H., Xu, S. et al. (2021). Tailoring multifunctional passivation molecules with halogen functional groups for efficient and stable perovskite photovoltaics. *Chemical Engineering Journal*, 407, 127204. DOI 10.1016/j.cej.2020.127204.